Hindawi
Geofluids
Volume 2022, Article ID 6711977, 12 pages
https://doi.org/10.1155/2022/6711977

Research Article

An Improved Model for Evaluating the Brittleness of Shale Oil Reservoirs Based on Dynamic Elastic Properties: A Case Study of Lucaogou Formation, Jimusar Sag

Yang Gao,[1,2] Yan Dong,[2] Lei Chen,[3] Yingyan Li,[2] Jianhua Qin,[2] and Zhenxue Jiang[1,3]

[1]*Unconventional Oil and Gas Research Institute, China University of Petroleum-Beijing, Beijing 102249, China*
[2]*Xinjiang Oilfield Company, PetroChina, Karamay, Xinjiang 834000, China*
[3]*State Key Laboratory of Petroleum Resources and Prospecting, China University of Petroleum-Beijing, Beijing 102249, China*

Correspondence should be addressed to Lei Chen; rawson163@163.com

Received 13 March 2022; Revised 14 April 2022; Accepted 20 April 2022; Published 4 May 2022

Academic Editor: Hasan N. Al-Saedi

Copyright © 2022 Yang Gao et al. This is an open access article distributed under the Creative Commons Attribution License, which permits unrestricted use, distribution, and reproduction in any medium, provided the original work is properly cited.

Rock brittleness is a critical factor affecting the stimulation of shale oil reservoirs. For efficient development of the shale oil in Lucaogou Formation, Jimusar Sag, the brittleness of the sweet spots needs to be evaluated. In this paper, the triaxial compression, acoustic wave measurements, and three-point bending tests were carried out on the reservoir cores. Based on the prepeak energy characteristics of the stress-strain curve, the brittleness of different horizons was calculated, with the largest difference of 24.89%. An improved model based on dynamic elastic properties was proposed to evaluate the brittleness along the vertical pay zones, by which the continuous brittleness in the upper sweet spot was found more changeful than that in the lower sweet spot. The linear correlation coefficient between the brittleness from the improved model and that from the laboratory tests is 0.85, improving the accuracy by 21% and 27% respectively, compared with the conventional elastic property methods. From the characteristics of compression fractures and the length of the fracture process zone, it was found that the compression fractures were more complex and the fracture process zone length was shorter in a more brittle rock, verifying the reliability of the improvement model. The improved method based on dynamic elastic properties proposed in this paper is expected to guide the brittleness evaluation in other regions.

1. Introduction

With the increasing demand for oil and gas, unconventional energy sources, shale oil being one principle contributor, have become the focus of exploration and development [1–4]. As an effective measure to stimulate the reservoirs [5–7], fracturing technology, especially the stimulated reservoir volume fracturing, has played an important role in the exploitation of shale oil, improving the production of shale oil [8]. In fracturing design, the brittleness of reservoir rocks is an important parameter of concern, providing guidance for evaluating the feasibility of reservoir fracturing [9]. It is generally believed that the brittleness of reservoir rock would affect the complexity of the fracture. That is, the more brittle the rock is, the more complex the hydraulic fracture is [10].

At present, there is no unified standard in the evaluation of rock brittleness [11]. The evaluation of reservoir rock brittleness is mainly from lithology analysis, geophysical methods, and rock mechanics experiments [12–16]. The methods based on lithologic characteristics consider the content of brittle minerals [17, 18]. However, the previous research shows that mineral compositions could not accurately reflect the brittleness of rocks [12, 17, 19]. In addition, the scholars hardly unanimously agree on the classification criteria for brittle minerals [18–20]. In the geophysical method, the rock porosity or mineral component distribution of formation needs to be predicted in advance [15, 16], without comparing with laboratory tests. Brittleness evaluation based on mechanical experiments can be assessed with stress-strain curve analysis, rock mechanical strength evaluation, and calculation of the elastic properties [14, 21–24],

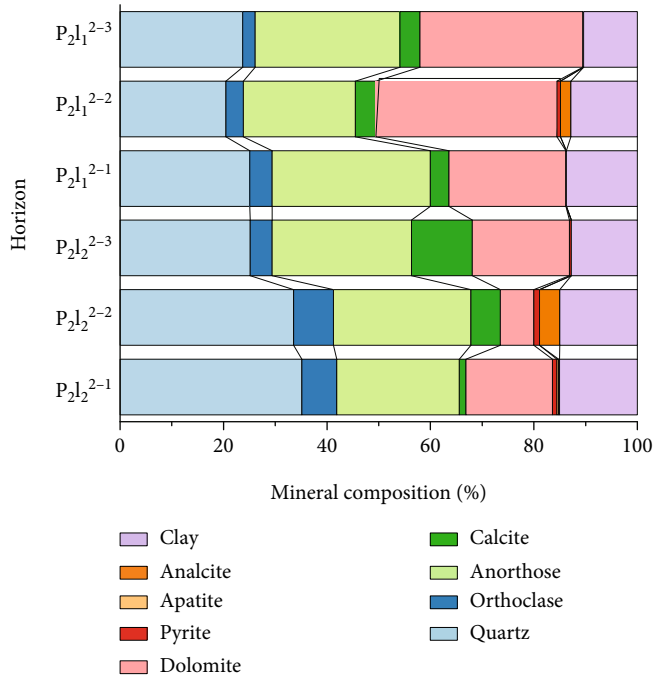

Figure 1: Mineral composition in different horizons.

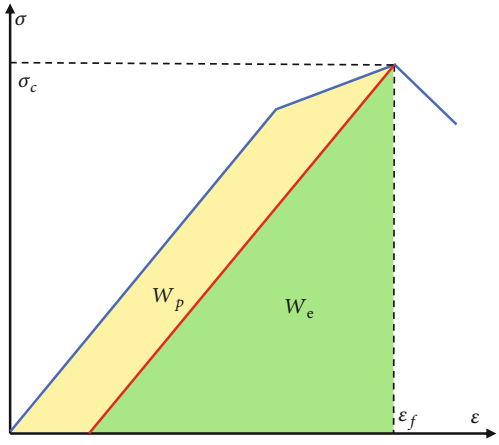

Figure 2: Evaluation of rock brittleness based on the prepeak energy.

among which the elastic property method is widely used [9]. The brittleness evaluation by rock mechanics would be limited by the number of specimen cores, so it is difficult to carry out the rock brittleness evaluation across the pay zones continuously. Therefore, it is necessary to evaluate the rock brittleness continuously using acoustic logging, where evaluating accuracy is an essential topic, especially those from elastic properties. The improvement of the evaluation method based on elastic properties still needs to be studied [9, 12].

The shale oil of Lucaogou Formation in Jimusar Sag, China, is a national demonstration area of continental shale, consisting of two sweet spots. With the characteristics of interlamination, the reservoirs are oil-bearing overall [25–28]. The rock mechanical properties of Lucaogou Formation present diversities in different horizons, and the factors influencing the complexity of hydraulic fractures remain to be studied. Especially when the sweet spots need to be developed as a whole, it is necessary to evaluate the stimulation feasibility of different horizons in the upper and lower sweet spots. The precondition for estimating the stimulation feasibility of reservoirs is the evaluation of brittleness [8, 29], especially the continuous brittleness.

In this paper, the reservoir cores of shale oil in Lucaogou Formation were selected to carry out the triaxial compression, acoustic wave, and three-point bending experiments. Based on the stress-strain curve, the brittleness of different horizons was evaluated. An improved model for evaluating the continuous brittleness by elastic properties was proposed, verified by the characteristics of compression fractures and the length of the fracture process zone. The improvement method proposed in this paper is expected to be a reference for the field when the brittleness needs to be estimated using acoustic logging data.

2. Geological Background

Jimusar Sag is located in the east of the Junggar Basin, China, bounded by the Santai Fault in the south and the Jimusar Fault in the north. It is a typical dustpan depression with depth in the west and shallowness in the east [25–28]. Shale oil in Jimusar Sag is mainly developed in the Permian Lucaogou Formation, which belongs to the continental liquid hydrocarbon shale, a typical representative of shale oil in the foreland salinized lake basin [25–28, 30]. Lucaogou Formation is simple in structure and stable in distribution. The formation thickness is 25 m~300 m, with an average of 200 m, and the buried depth is 800 m-4800 m, with an

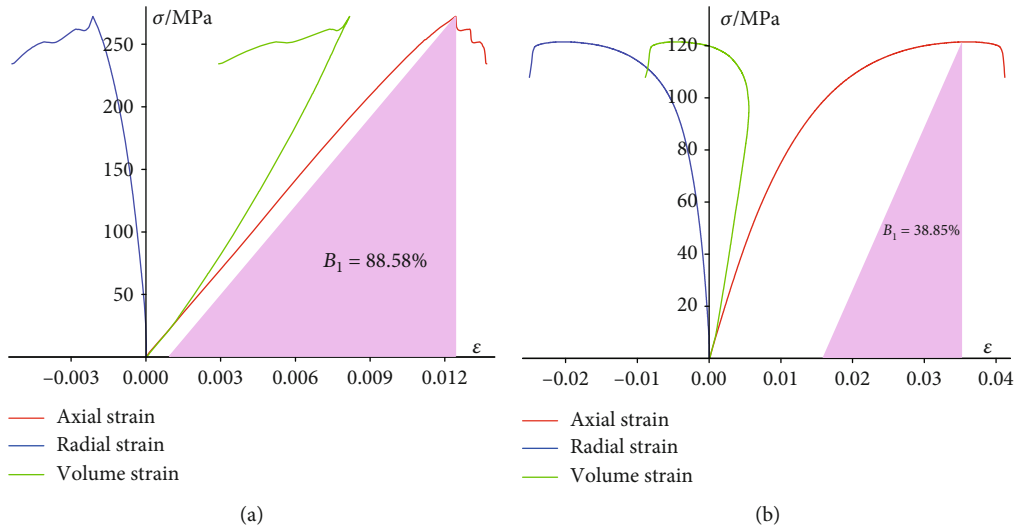

Figure 3: Typical stress-strain curves of higher and lower brittle rocks.

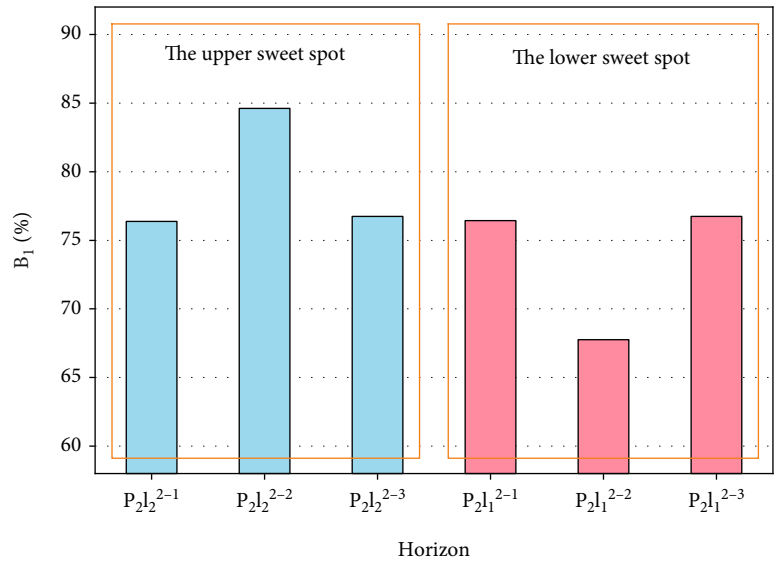

Figure 4: The brittleness distribution in different horizons.

average of 3570 m. Affected by the multisource mixed accumulation of volcanic rocks, clastic rocks, and carbonate rocks, the lithology of the reservoir is diverse, mainly including mudstone, fine silty sandstone, and microcrystalline dolomite [30].

The shale oil in the Lucaogou Formation is concentrated in two sections, where two sweet spots are developed with high porosity and stable distribution [30]. The upper sweet spot ($P_2l_2^2$) can be divided into three horizons ($P_2l_2^{2\text{-}1}$, $P_2l_2^{2\text{-}2}$, and $P_2l_2^{2\text{-}3}$), of which the superposition thickness is more than 18 m. The lower sweet spot ($P_2l_1^2$) can be divided into six horizons ($P_2l_1^{2\text{-}1}$~$P_2l_1^{2\text{-}6}$), but the oil is intensively developed in $P_2l_1^{2\text{-}1}$~$P_2l_1^{2\text{-}3}$, where the superposition thickness of the main area is greater than 17 m. The mineral composition analysis using X-ray diffraction was carried out on the rock cores of the Lucaogou Formation in Jimusar Sag. As shown in Figure 1, it is found that the rock mineral compositions of the upper and lower sweet spots are relatively similar, mainly including quartz, feldspar, calcite, dolomite, and clay.

3. Methods and Results in the Evaluation of Brittleness

3.1. Evaluation of Brittleness Based on the Prepeak Energy. In recent years, calculating the energy characteristics of the compression stress-strain curve has been a reasonable way to evaluate rock brittleness [19, 22, 31–36]. Some scholars used prepeak energy to evaluate rock brittleness from the stress-strain curve [36], describing the proportion of accumulative plastic energy [36]. Some scholars believe that estimating postpeak instability based on postpeak energy balance is a means to characterize rock brittleness [22]. In recent publications, the brittleness also was evaluated by

prepeak and postpeak energies [19]. At present, there is no consensus on which method is the most reliable [19, 22, 31–36]. In the postpeak methods, the characteristics of fracture generated after the peak would affect the pattern of the post stress-strain curve. Thus, we adopted the characteristics of prepeak energy [36] to calculate the rock brittleness of the Lucaogou Formation, which is more representative to evaluate the accumulation of elastic energy before failure.

As shown in Figure 2, during the process of rock compression, elastic deformation and plastic deformation would be generated. The elastic energy W_e together with elastic deformation is recoverable stored energy, and the plastic energy W_p during the plastic process is unrecoverable consumption energy. Previous studies show that dissipated energy W_p is an important parameter to measure the plastic characteristics of rock. The greater the W_p proportions, the more obvious the plastic characteristics would be, so the brittleness of the rock is lower, and the larger the W_e proportions, the greater the stored energy is, so the rock would be more brittle. The calculation of brittleness is shown in the following equation [36].

$$B_1 = \frac{W_e}{W_e + W_p}, \tag{1}$$

where B_1 is the brittleness index based on the prepeak energy of the stress-strain curve, W_e the elastic energy, and W_p the plasticity energy.

Figures 3(a) and 3(b) are the typical stress-strain curves of higher and lower brittleness of shale oil in the Lucaogou Formation. We could find that the elastic stage is dominant of the stress-strain curve in Figure 3(a), where the brittleness index is 88.58%. The stress-strain curve in Figure 3(b) presents prominent plastic characteristics, where the brittleness index is only 38.85%.

Based on Equation (1), the brittleness of shale oil among different horizons in Lucaogou Formation was obtained, as shown in Figure 4, and it was found that there were significant differences in rock brittleness of different horizons in the upper and lower sweet spots. In the upper sweet spot, the brittleness index of $P_2l_2^{2\text{-}2}$ is the largest, which is 84.61%. The brittleness index of $P_2l_1^{2\text{-}2}$ is smallest in the lower sweet spot, reaching 67.75%, and the brittleness of $P_2l_2^{2\text{-}1}$, $P_2l_2^{2\text{-}3}$, $P_2l_1^{2\text{-}1}$, and $P_2l_1^{2\text{-}3}$ is close, about 76%. The current fracturing practice of the upper sweet spot shows that shale oil production in the $P_2l_2^{2\text{-}2}$ horizon is best [37], which is consistent with the brittleness calculation results, indicating the rationality of brittleness evaluation on the characteristics of prepeak energy.

3.2. The Improved Brittleness Evaluation Model Based on Dynamic Elastic Properties. In the brittleness evaluation based on mechanical parameters, some scholars have found that there is a close relationship between rock brittleness and elastic modulus and Poisson's ratio: the rock would be more brittle when the elastic modulus is larger, and the Poisson's ratio is smaller, and the rock brittleness could be calculated as in Equation (2) [38] and Equation

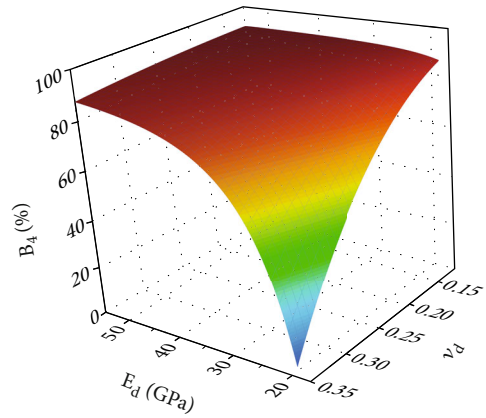

Figure 5: The three-dimensional function relationship of B_4, E_d, and ν_d.

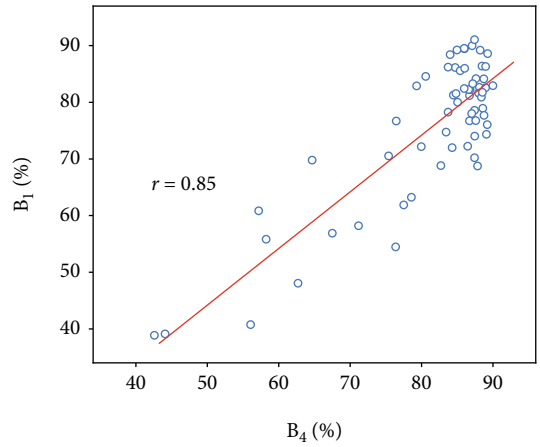

Figure 6: Linear relation between B_4 and B_1.

(3) [39], which could be called elastic property methods. Although the rock brittleness is related to the elastic constant [38–40], the present methods based on elastic properties were suspicious for the lack of comparison with other methods. The weighted average calculation of the elastic modulus and Poisson's ratio in Equation (2) lacks a theoretical basis, and the calculated value in Equation (3) will be unstable with the change of elastic constant [39]. Therefore, these two methods have been questioned by scholars [9, 12, 39].

$$B_2 = \frac{1}{2}\left(\frac{E - E_{\min}}{E_{\max} - E_{\min}} + \frac{\nu - \nu_{\max}}{\nu_{\min} - \nu_{\max}}\right) \times 100\%, \tag{2}$$

$$B_3 = \frac{E}{\nu} \times 100\%, \tag{3}$$

where E is the modulus of elasticity, $E_{\max}$ is the largest value of elastic modulus in the measured area, $E_{\min}$ the smallest value of elastic modulus, ν is the Poisson's ratio, $V_{\max}$ is the largest value of the Poisson's ratio, and $V_{\min}$ is the smallest value of the Poisson's ratio.

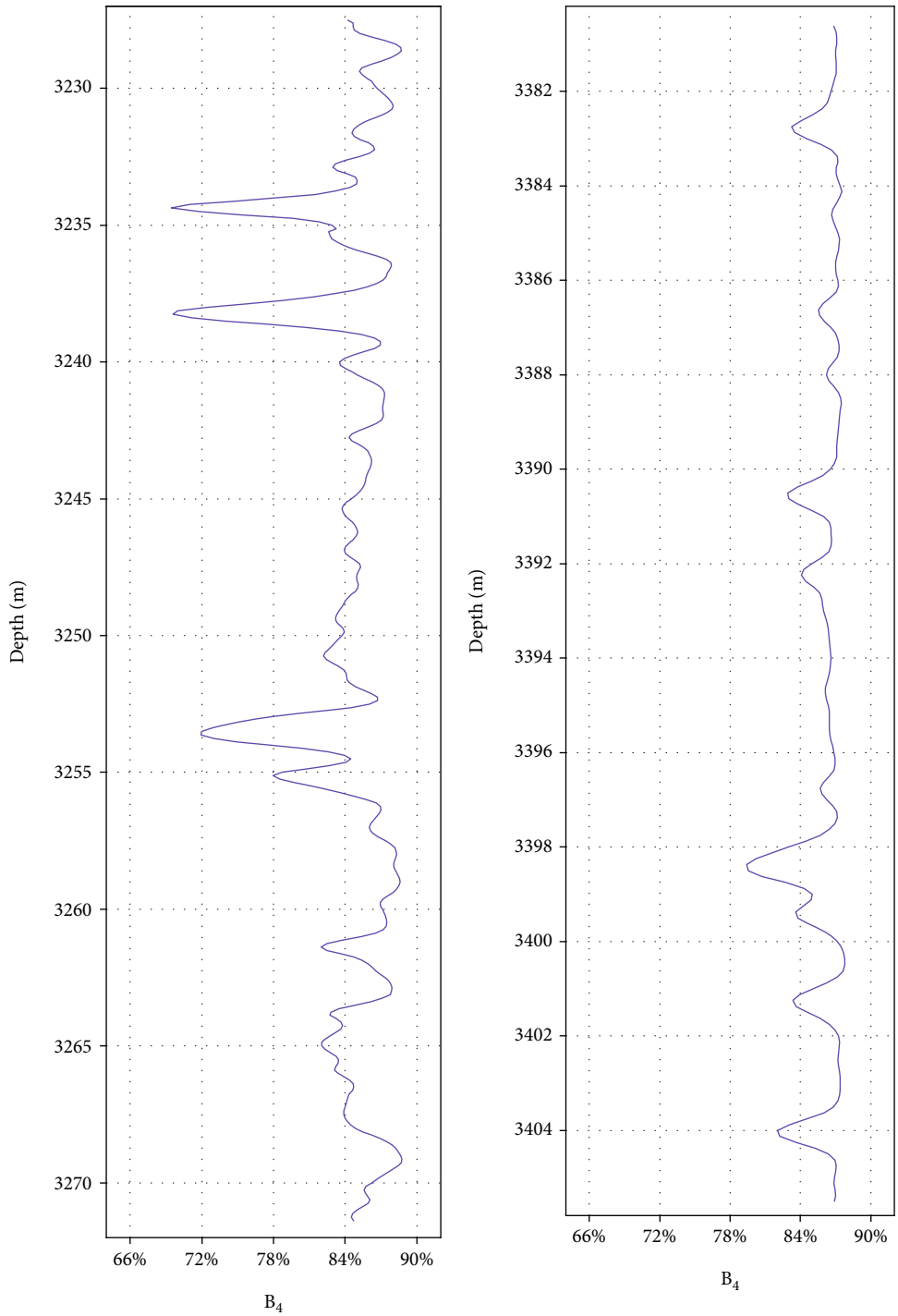

(a) The upper sweet spot of well J10014

(b) The lower sweet spot of well J10014

Figure 7: Continued.

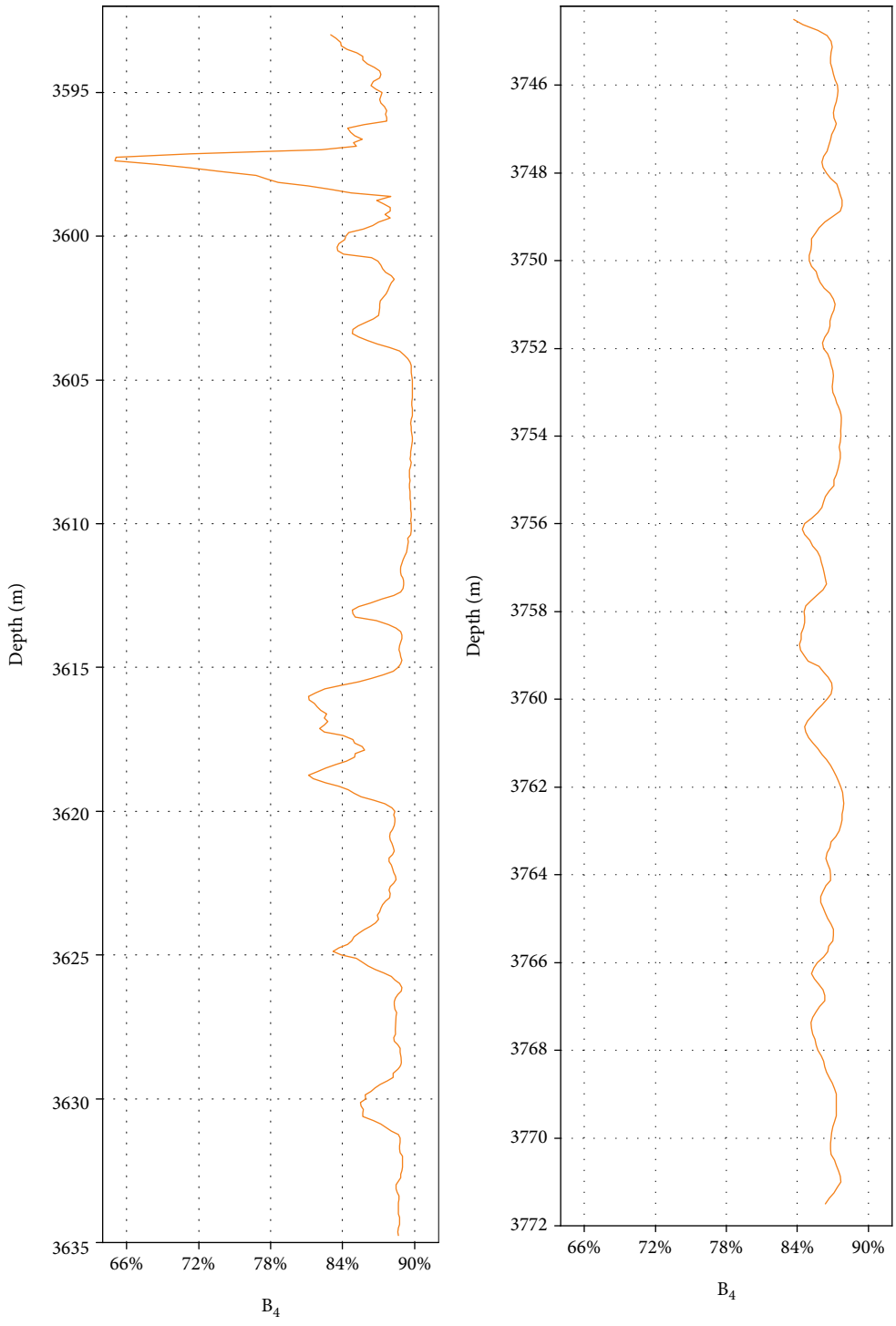

(c) The upper sweet spot of well J251

(d) The lower sweet spot of well J251

Figure 7: The vertical distribution of brittleness in wells J10014 and J251.

Although shortcomings exist in the present evaluation methods using elastic properties, the technique of brittleness evaluation based on elastic properties has significant advantages. Especially in the brittleness evaluation via acoustic logging data, a reasonable brittleness calculation model can provide bases for evaluating the continuous brittleness of reservoirs.

Exploring the relationship between dynamic elastic constant and brittleness of rocks could provide proper support for brittleness calculation from field acoustic logging data. The acoustic parameters of rock cores were tested, and the dynamic elastic modulus and dynamic Poisson's ratio were calculated from Equations (4) and (5) [41]. Referring to the previous research on the

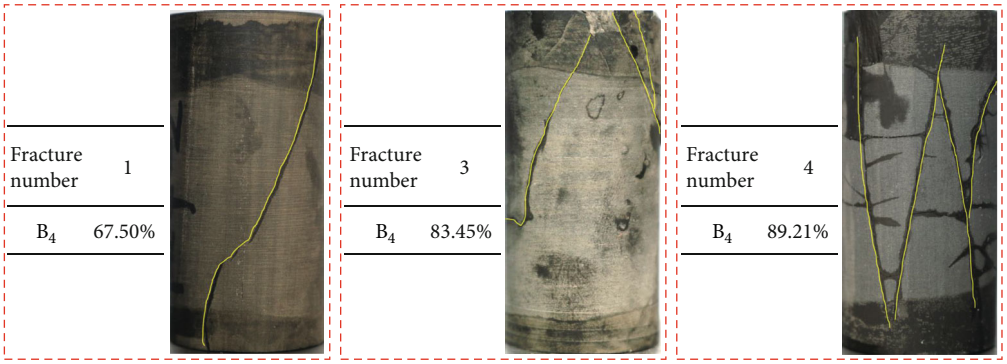

Figure 8: The typical fracture characteristics of shale oil cores after failure.

relationship of elastic constant and brittleness [38, 39], a three-parameter model for calculating the factor of rock brittleness was proposed in this paper, as shown in Equation (6), where α is related to the influence of the dynamic Poisson's ratio on brittleness and β would decide the proportion of the dynamic elastic modulus.

$$E_d = \frac{\rho V_s^2\left(3V_p^2 - 4V_s^2\right)}{V_p^2 - V_s^2}, \tag{4}$$

$$v_d = \frac{\left(V_p/V_s\right)^2 - 2}{2\left[\left(V_p/V_s\right)^2 - 1\right]}, \tag{5}$$

$$F_d = \alpha E_d^{\beta} v_d^{\gamma}, \tag{6}$$

where V_p is the longitudinal wave velocity, V_s the shear wave velocity, ρ the density of rock sample, E_d the dynamic elastic modulus, v_d the dynamic Poisson's ratio, F_d the rock brittleness evaluation factor, and α, β, γ the relevant parameters for calculating rock brittleness.

In the three-parameter model for evaluating the brittleness factor, determining the values of the three parameters is the key. In order to improve the accuracy of brittleness evaluation based on dynamic elastic properties, the global optimization method was used to solve the parameters in this paper, aimed at the consistency with the results by the energy method. We defined r as the correlation coefficient between B_1 and F_d, as in Equation (7), where r is an equation containing parameters α, β, γ. If the brittleness evaluation model based on dynamic elastic constant was expected to present high consistency with the energy method, the correlation coefficient r should be sufficiently large. During the solution of parameters based on the global optimization algorithm, the optimal solution of α, β, γ could be obtained when r reaches the maximum value in Equation (8).

In this paper, the maximum value of the correlation coefficient r is found to be 0.85 when α is -2.478, β is -2.77, and γ is 2.65. The improved brittleness evaluation model based on dynamic elastic properties is shown in Equation (9). For the shale oil of Lucaogou Formation in Jimusar Sag, the brittleness evaluation model is shown in Equation (10).

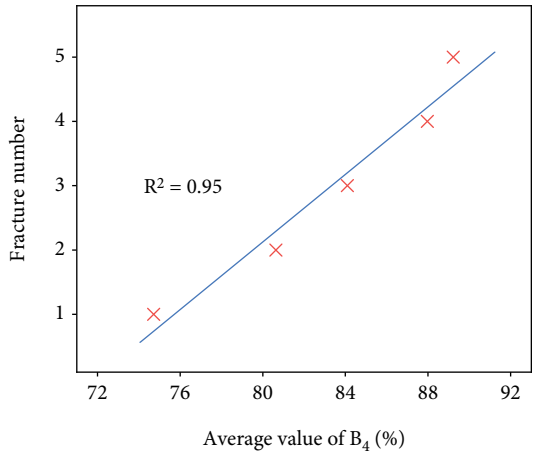

Figure 9: The relationship between B_4 and fracture number.

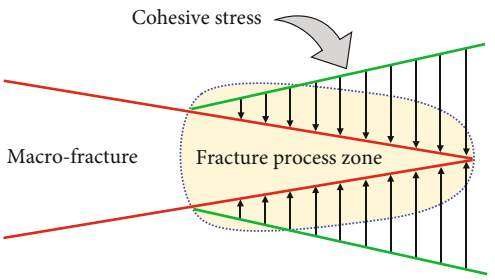

Figure 10: The fracture process zone ahead of the fracture.

$$r = \frac{\mathrm{Cov}(B_1, F_d)}{\sqrt{\mathrm{Var}[B_1]\mathrm{Var}[F_d]}}, \tag{7}$$

$$r_{\max} = f\left(\alpha_{\mathrm{opt}}, \beta_{\mathrm{opt}}, \gamma_{\mathrm{opt}}\right), \tag{8}$$

$$B_4 = B_{1m} + kF_d, \tag{9}$$

$$B_4 = 91.04\% - 49190E_d^{-2.77}v_d^{2.65}, \tag{10}$$

where r is the correlation coefficient of B_1 and F_d; α_{opt}, β_{opt}, and γ_{opt} are the optimized solutions of the corresponding parameters; B_4 is the calculated value of brittleness based

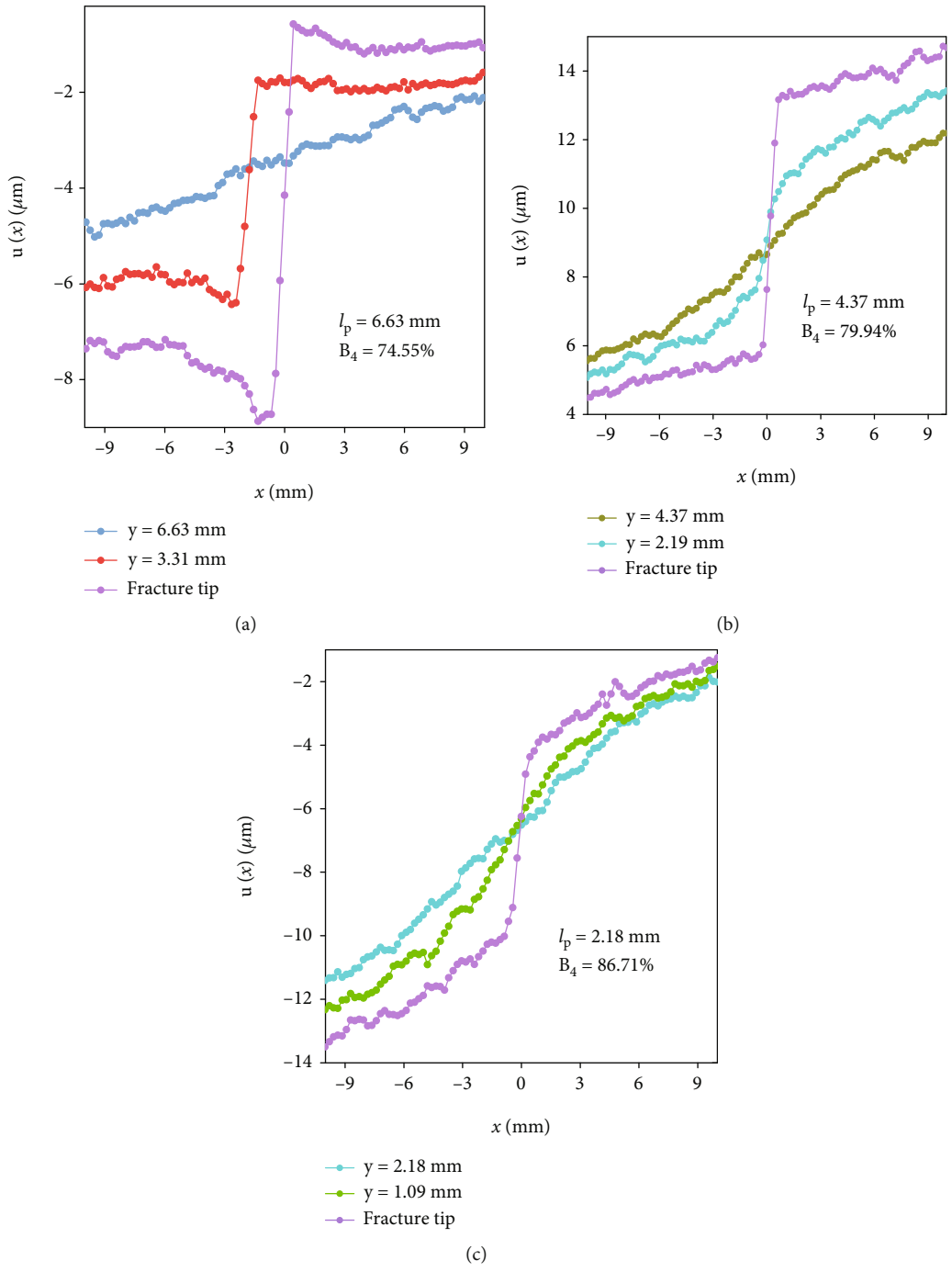

Figure 11: Characterization of the length of fracture process zone in different brittle rocks.

on the improved brittleness evaluation model; k is the linear fitting slope of B_1 and F_d; and B_{1m} is the extreme value of energy method (when α is positive, B_{1m} is the minimum value; when α is negative, B_{1m} is the maximum value).

Figure 5 shows the three-dimensional function relationship of B_4, E_d, and ν_d, drawn by the improved brittleness evaluation model based on dynamic elastic properties. It could be found that the brittleness index would increase when the elastic modulus increases and the Poisson's ratio decreases, consistent with the previous opinions. However, the influence of elastic properties on brittleness is nonlinear. In this paper, we discover the effects of the dynamic elastic properties on the brittleness index intuitively from the improved model.

Figure 6 is the relationship between B_4 calculated by the improved brittleness evaluation model and B_1 calculated by the energy method, where a significant linear correlation relationship could be found, with a correlation coefficient of 0.85, indicating the reliability of the improved brittleness evaluation model based on dynamic elastic properties.

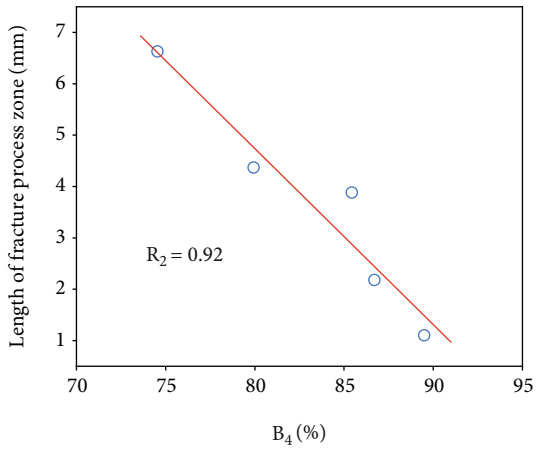

FIGURE 12: The relationship between B_4 and the length of the fracture process zone in Lucaogou Formation.

3.3. Application of the Brittleness Evaluation Model. In the previous section, an improved brittleness evaluation model based on dynamic elastic properties is proposed, providing a basis to evaluate the continuous brittleness distribution of reservoirs through acoustic logging data. Taking two wells in the Jimusar Sag as examples, we evaluated the continuous brittleness of shale oil in the Lucaogou Formation. When calculating the dynamic elastic properties of reservoirs, the relationship between the P-wave and the S-wave needs to be determined since the acoustic wave measured by acoustic logging is mainly P-wave. In this paper, through the indoor acoustic test, it is found that there is a significant linear relationship between the P-wave and the S-wave in the Lucaogou Formation. The relationships in the upper and lower sweet spots are shown in Equations (11) and (12), where r^2 are 0.83 and 0.82, respectively.

$$V_s = 0.5246V_p + 217.3816, \tag{11}$$

$$V_s = 0.5072V_p + 294.9584. \tag{12}$$

Well J10014 and well J251 were selected to analyze the longitudinal brittleness of the upper and lower sweet spots in the Lucaogou Formation. The dynamic elastic properties were calculated continuously based on the acoustic logging data, and then, the brittleness distribution of well J10014 and well J251 in different sweet spots could be obtained, as shown in Figure 7. By comparing the brittleness distribution of the upper and lower sweet spots, we could find that the vertical variation range of the brittleness index in the upper sweet spot is larger than that in the lower sweet spot.

4. Discussion

The improved brittleness evaluation model proposed in this paper could calculate the continuous brittleness of reservoirs through acoustic logging data. Compared with the conventional method of brittleness calculation based on elastic properties [38, 39], we found that the correlation coefficients between B_1 and B_2/B_3 were only 0.70 and 0.67, respectively, and the accuracy of the brittleness calculated by the improved model was improved by 21% and 27%, respectively. However, the reliability of the improved brittleness evaluation model still needs to be verified and discussed by mechanical experiments.

4.1. The Characteristics of Compression Fractures in Different Brittle Rocks. Conventional understanding believes that the brittleness index of rock would affect the complexity of the hydraulic fractures: the more brittle the rock is, the more complex the fractures are [10, 29]. To study the relationship between the fracture complexity and the brittleness index calculated by the improved model, we characterize the fracture complexity by the number of compression failure fractures in this paper. As in Figure 8, differences of compression fracture complexity exist in different brittle specimens of the Lucaogou Formation.

Based on the statistics of specimens, the number of compression failure fractures in the Lucaogou Formation is generally between 1 and 5. We calculated the average value of the brittleness index B_4 from core samples with the same number of compression failure fractures. As shown in Figure 9, there is a significant positive correlation between B_4 and the number of fractures. That is to say, the more brittle the rock is, the more complex the fractures are, verifying the reliability of the improved model in evaluating rock brittleness.

4.2. The Length of Fracture Process Zone in Different Brittle Rocks. The fracture process zone is a nonlinear development zone in front of the macrofracture, which could be regarded as a plastic zone roughly [42–45]. In the hydraulic fracturing of reservoirs, the fracture process zone will be generated ahead of the hydraulic fracture, as shown in Figure 10. There would be energy consumption in the development of the fracture process zone so that the energy consumption will increase with the length of the FPZ. The previous research indicates that the fracture process zone length is the inverse index of brittleness [46], and the longer the rock fracture process zone is, the lower the brittleness is. Although the monitoring and identification of the fracture process zone are complex, compared with other methods, the fracture process zone length could accurately reflect the brittleness of the rock.

In this paper, the reservoir cores with different brittleness indexes calculated by the optimization model were selected to carry out three-point bending fracture tests. The digital image correlation method was used to monitor the fracture process in real time, and the displacements of the specimens were calculated by an open-source program [47]. Based on the existing methods, the fracture process zone length of reservoir rocks was identified by the characteristics of horizontal displacement [48–50]. And the typical fracture process zone lengths of Lucaogou Formation rocks with different brittleness B_4 were characterized in Figure 11, where the length of the fracture process zone is larger when the rock brittleness evaluated by the improvement model is smaller.

A linear relation could be found from B_4 and the length of fracture process zone (Figure 12), providing a basis to evaluate the fully developed length of the fracture process zone of the Lucaogou Formation using acoustic logging, as in Equation (13). Previous studies show that the length of the fracture process zone is related to the fracture energy [46], indicating that more energy would be consumed in a longer process zone. The experimental results mean that B_4 is negatively correlated with the dissipated energy, verifying the reliability of the improved brittleness evaluation model based on dynamic elastic properties.

$$l_p = 32.16 - 34.27B_4 \ (B_4 < 91.04\%). \quad (13)$$

5. Conclusion

In this paper, the reservoir cores of shale oil in the Lucaogou Formation, Jimusar Sag, were selected to carry out the triaxial compression, acoustic wave, and three-point bending tests. Based on the prepeak energy characteristics of the triaxial stress-strain curve, the brittleness index of different horizons in the upper and lower sweet spots was calculated. The improved model based on dynamic elastic properties was proposed to evaluate the continuous brittleness of reservoirs, verified by the compression fracture characteristics and the length of the fracture process zone, and the following conclusions are obtained.

(1) From the calculated results of rock brittleness, it is found that differences exist among horizons in the upper and lower sweet spots. The brittleness index of $P_2l_2^{2\text{-}2}$ is the largest in the upper sweet spot, which is 84.61%, and the brittleness index of $P_2l_1^{2\text{-}2}$ is the smallest in the lower, reaching 67.75%. The continuous brittleness in the Lucaogou Formation calculated by acoustic logging data shows that the vertical variation in the upper sweet spot is more significant than the lower

(2) A brittleness evaluation model based on dynamic elastic properties was proposed after the optimization of parameters. The linear correlation coefficient of the brittleness calculated by the improved model and the energy method is 0.85, which improves the accuracy of brittleness evaluation by 21% and 27%, respectively, compared with the results by the conventional evaluation methods from elastic properties

(3) The improved brittleness evaluation model was verified by the results of mechanical experiments, where the compression fractures would be more complex when the brittleness index is larger. The relationship between B_4 and the length of the fracture process zone obtained by experiments presents a linear negative correlation, indicating the reliability of the improved model

Data Availability

The data used to support the findings of this study are included within the article.

Conflicts of Interest

The authors declare that they have no conflicts of interest.

Acknowledgments

This study was supported by the Xinjiang Major Science and Technology Special Projects of China National Petroleum Corporation: Research and Application of Key Technologies in the Exploration and Development of Continental Medium and High Maturity Level Shale Oil (2019E-2607), Integration and Testing of Crucial Engineering Technologies in Horizontal Wells for the Efficient Development of Shale Oil in Jimusar, National Demonstration Area (2020F-50).

References

[1] Z. Kang, Z. Wang, Y. Lu, R. Cao, D. Huang, and Q. Meng, "Investigation on the effect of atmosphere on the pyrolysis behavior and oil quality of Jimusar oil shale," *Geofluids*, vol. 2022, Article ID 1408690, 9 pages, 2022.

[2] M. O. Eshkalak, S. D. Mohaghegh, and S. Esmaili, "Geomechanical properties of unconventional shale reservoirs," *Journal of Petroleum Engineering*, vol. 2014, 10 pages, 2014.

[3] B. Liu, A. Bechtel, R. F. Sachsenhofer, D. Gross, R. Gratzer, and X. Chen, "Depositional environment of oil shale within the second member of Permian Lucaogou Formation in the Santanghu Basin, Northwest China," *International Journal of Coal Geology*, vol. 175, pp. 10–25, 2017.

[4] B. Liu, H. Wang, X. Fu et al., "Lithofacies and depositional setting of a highly prospective lacustrine shale oil succession from the Upper Cretaceous Qingshankou Formation in the Gulong sag, northern Songliao Basin, Northeast China," *American Association of Petroleum Geologists Bulletin*, vol. 103, no. 2, pp. 405–432, 2019.

[5] Z. Z. Le, G. Q. Zhang, H. R. Dong, L. Z. Bin, and Y. X. Nie, "Creating a network of hydraulic fractures by cyclic pumping," *International Journal of Rock Mechanics and Mining Sciences*, vol. 97, no. 97, pp. 52–63, 2017.

[6] L. Chen, G. Zhang, Y. Lyu, Z. Li, and X. Zheng, "Visualization study of hydraulic fracture propagation in unconsolidated sandstones," in *53rd US rock mechanics/geomechanics symposium*, New York City, June 2019.

[7] D. Zhou, G. Zhang, Y. Wang, and Y. Xing, "Experimental investigation on fracture propagation modes in supercritical carbon dioxide fracturing using acoustic emission monitoring," *International Journal of Rock Mechanics and Mining Sciences*, vol. 110, pp. 111–119, 2018.

[8] J. Li, Y. Zou, S. Shi et al., "Experimental study on fracture propagation mechanism of shale oil reservoir of Lucaogou Formation in Jimusar," *Geofluids*, vol. 2022, Article ID 6598575, 11 pages, 2022.

[9] R. Rickman, M. Mullen, E. Petre, B. Grieser, and D. Kundert, "A practical use of shale petrophysics for stimulation design optimization: all shale plays are not clones of the Barnett Shale," in *SPE annual technical conference and exhibition*, vol. 2, pp. 840–850, Denver, Colorado, USA, Sep. 2008.

[10] S. Kahraman and R. Altindag, "A brittleness index to estimate fracture toughness," *International Journal of Rock Mechanics and Mining Sciences*, vol. 41, no. 2, pp. 343–348, 2004.

[11] K. K. Chong, W. V. Grieser, A. Passman, C. H. Tamayo, N. Modeland, and B. Burke, "A completions guide book to shale-play development: a review of successful approaches towards shale-play stimulation in the last two decades," in *Canadian unconventional resources and international petroleum conference*, Calgary, Alberta, Canada, October 2010.

[12] F. Meng, L. N. Y. Wong, and H. Zhou, "Rock brittleness indices and their applications to different fields of rock engineering: a review," *Journal of Rock Mechanics and Geotechnical Engineering*, vol. 13, no. 1, pp. 221–247, 2021.

[13] Y. Xia, H. Zhou, C. Zhang, S. He, Y. Gao, and P. Wang, "The evaluation of rock brittleness and its application: a review study," *European Journal of Environmental and Civil Engineering*, vol. 26, no. 1, pp. 239–279, 2022.

[14] B. Hou, Y. Zeng, M. Fan, and D. Li, "Brittleness evaluation of shale based on the Brazilian splitting test," *Geofluids*, vol. 2018, 11 pages, 2018.

[15] X. Jin, S. Shah, J. Truax, and J.-C. Roegiers, "A practical petrophysical approach for brittleness prediction from porosity and sonic logging in shale reservoirs," in *SPE annual technical conference and exhibition*, Amsterdam, The Netherlands, October 2014.

[16] M. Heidari, G. R. Khanlari, M. Torabi-Kaveh, S. Kargarian, and S. Saneie, "Effect of porosity on rock brittleness," *Rock Mechanics and Rock Engineering*, vol. 47, no. 2, pp. 785–790, 2014.

[17] D. M. Jarvie, R. J. Hill, T. E. Ruble, and R. M. Pollastro, "Unconventional shale-gas systems: the Mississippian Barnett Shale of North-Central Texas as one model for thermogenic shale-gas assessment," *American Association of Petroleum Geologists Bulletin*, vol. 91, no. 4, pp. 475–499, 2007.

[18] A. Hofmann, C. Rigollet, E. Portier, and S. Burns, "Gas shale characterization-results of the mineralogical, lithological and geochemical analysis of cuttings samples from radioactive Silurian Shales of a Palaeozoic Basin, SW Algeria," in *North Africa Technical Conference and Exhibition*, Cairo, Egypt, April 2013.

[19] B. Liu, S. Wang, X. Ke et al., "Mechanical characteristics and factors controlling brittleness of organic-rich continental shales," *Journal of Petroleum Science and Engineering*, vol. 194, article 107464, 2020.

[20] R. Sierra, M. H. Tran, Y. N. Abousleiman, and R. M. Slatt, "Woodford shale mechanical properties and the impacts of lithofacies," in *44th US rock mechanics symposium and 5th US-Canada rock mechanics symposium*, Salt Lake City, Utah, June 2010.

[21] D. Zhang, P. G. Ranjith, and M. S. A. Perera, "The brittleness indices used in rock mechanics and their application in shale hydraulic fracturing: a review," *Journal of Petroleum Science and Engineering*, vol. 143, pp. 158–170, 2016.

[22] B. Tarasov and Y. Potvin, "Universal criteria for rock brittleness estimation under triaxial compression," *International Journal of Rock Mechanics and Mining Sciences*, vol. 59, pp. 57–69, 2013.

[23] R. Nygård, M. Gutierrez, R. K. Bratli, and K. Høeg, "Brittle-ductile transition, shear failure and leakage in shales and mudrocks," *Marine and Petroleum Geology*, vol. 23, no. 2, pp. 201–212, 2006.

[24] S. Yagiz, "Assessment of brittleness using rock strength and density with punch penetration test," *Tunnelling and Underground Space Technology*, vol. 24, no. 1, pp. 66–74, 2009.

[25] C. Zhang, J. Cao, E. Li, Y. Wang, W. Xiao, and Y. Qin, "Revisiting controls on shale oil accumulation in saline lacustrine basins: the Permian Lucaogou Formation mixed rocks, Junggar Basin," *Geofluids*, vol. 2021, 25 pages, 2021.

[26] J. Lu, C. Zhang, J. Zeng, and H. Yuan, "Research on the oil-bearing difference of bedding fractures: a case study of Lucaogou Formation in Jimsar Sag," *Geofluids*, vol. 2021, 21 pages, 2021.

[27] L. Hou, X. Luo, Z. Zhao, and L. Zhang, "Identification of oil produced from shale and tight reservoirs in the Permian Lucaogou Shale sequence, Jimsar Sag, Junggar Basin, NW China," *ACS Omega*, vol. 6, no. 3, pp. 2127–2142, 2021.

[28] X. Wang, Y. Song, X. Guo et al., "Pore-throat structure characteristics of tight reservoirs of the Middle Permian Lucaogou formation in the Jimsar Sag, Junggar Basin, Northwest China," *Journal of Petroleum Science and Engineering*, vol. 208, p. 109245, 2022.

[29] H. Shimizu, T. Ito, T. Tamagawa, and K. Tezuka, "A study of the effect of brittleness on hydraulic fracture complexity using a flow-coupled discrete element method," *Journal of Petroleum Science and Engineering*, vol. 160, pp. 372–383, 2018.

[30] Y. Zhi, H. Lianhua, L. Senhu et al., "Geologic characteristics and exploration potential of tight oil and shale oil in Lucaogou Formation in Jimsar Sag," *China Petroleum Exploration*, vol. 23, no. 4, pp. 76–85, 2018.

[31] B. G. Tarasov, "Superbrittleness of rocks at high confining pressure," in *Proceedings of the Fifth International Seminar on Deep and High Stress Mining*, pp. 119–133, Perth, Australian, 2010.

[32] B. G. Tarasov and M. F. Randolph, "Superbrittleness of rocks and earthquake activity," *International Journal of Rock Mechanics and Mining Sciences*, vol. 48, no. 6, pp. 888–898, 2011.

[33] W. Jb and W. F. Brace, "A fracture criterion for brittle anisotropic rock," *Journal of Geophysical Research*, vol. 69, no. 16, pp. 3449–3456, 1964.

[34] W. R. Wawersik and C. H. Fairhurst, "A study of brittle rock fracture in laboratory compression experiments," *International Journal of Rock Mechanics and Mining Sciences & Geomechanics Abstracts*, vol. 7, no. 5, pp. 561–575, 1970.

[35] L. I. Baron, B. M. Loguntsov, and I. Z. Posin, *Determination of rock properties*, NTILGD. Published online, Moscow, 1962.

[36] V. Hucka and B. Das, "Brittleness determination of rocks by different methods," *International Journal of Rock Mechanics and Mining Sciences*, vol. 11, no. 10, pp. 389–392, 1974.

[37] W. Baocheng, L. Jianmin, W. Yuanyue, H. Le, Z. Tingfeng, and Z. Yushi, "Development practices of geology-engineering integration on upper sweet spots of Lucaogou Formation shale oil in Jimsar Sag, Junggar Basin," *China Petroleum Exploration*, vol. 24, no. 5, pp. 679–690, 2019.

[38] W. V. Grieser and J. M. Bray, "Identification of production potential in unconventional reservoirs," in *Production and Operations Symposium*, Oklahoma City, Oklahoma, U.S.A, March 2007.

[39] Z. Liu and Z. Sun, "New brittleness indexes and their application in shale/clay gas reservoir prediction," *Petroleum Exploration and Development*, vol. 42, no. 1, pp. 117–124, 2015.

[40] B. Liu, K. Liu, A. Abarghani et al., "1D mechanical earth modeling in the Permian Lucaogou Shale of the Santanghu Basin, Northwest China, from a complete set of laboratory data," *Interpretation*, vol. 9, no. 2, pp. T357–T372, 2021.

[41] N. A. Al-Shayea, "Effects of testing methods and conditions on the elastic properties of limestone rock," *Engineering Geology*, vol. 74, no. 1-2, pp. 139–156, 2004.

[42] L. Chen, G. Zhang, Z. Zou, Y. Guo, and X. Zheng, "The effect of fracture growth rate on fracture process zone development in quasi-brittle rock," *Engineering Fracture Mechanics*, vol. 258, p. 108086, 2021.

[43] L. Chen, G. Zhang, Z. Zou, Y. Guo, and X. Du, "Experimental observation of fracture process zone in sandstone from digital imaging," in *54th US Rock Mechanics/Geomechanics Symposium*, Golden, Colorado, USA, June 2020.

[44] Y. Xing, B. Huang, E. Ning, L. Zhao, and F. Jin, "Quasi-static loading rate effects on fracture process zone development of mixed-mode (I-II) fractures in rock-like materials," *Engineering Fracture Mechanics*, vol. 240, p. 107365, 2020.

[45] Y. Xing and B. Huang, "Injection rate-dependent deflecting propagation rule of hydraulic fracture: insights from the rate-dependent fracture process zone of mixed-mode (I-II) fracturing," *Geofluids*, vol. 2021, Article ID 8199095, 17 pages, 2021.

[46] M. Elices, G. V. Guinea, J. Gómez, and J. Planas, "The cohesive zone model: advantages, limitations and challenges," *Engineering Fracture Mechanics*, vol. 69, no. 2, pp. 137–163, 2002.

[47] J. Blaber, B. Adair, and A. Antoniou, "Ncorr: open-source 2D digital image correlation Matlab software," *Experimental Mechanics*, vol. 55, no. 6, pp. 1105–1122, 2015.

[48] Q. Lin and J. F. Labuz, "Fracture of sandstone characterized by digital image correlation," *International Journal of Rock Mechanics and Mining Sciences*, vol. 60, pp. 235–245, 2013.

[49] Y. Nie, G. Zhang, Y. Xing, and S. Li, "Influence of water-oil saturation on the fracture process zone: a modified Dugdale-Barenblatt model," *Energies*, vol. 11, no. 11, p. 2882, 2018.

[50] G. Zhang, Y. Xing, and L. Wang, "Comprehensive sandstone fracturing characterization: integration of fiber Bragg grating, digital imaging correlation and acoustic emission measurements," *Engineering Geology*, vol. 246, pp. 45–56, 2018.